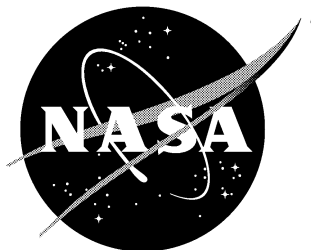


NASA/CR-2002-211430



Experiments With Fixed and Adaptive Herschel-Quincke Waveguides on the Pratt and Whitney JT15D Engine

*Jerome P. Smith and Ricardo A. Burdisso
Virginia Polytechnic Institute and State University
Blacksburg, Virginia*

March 2002

The NASA STI Program Office . . . in Profile

Since its founding, NASA has been dedicated to the advancement of aeronautics and space science. The NASA Scientific and Technical Information (STI) Program Office plays a key part in helping NASA maintain this important role.

The NASA STI Program Office is operated by Langley Research Center, the lead center for NASA's scientific and technical information. The NASA STI Program Office provides access to the NASA STI Database, the largest collection of aeronautical and space science STI in the world. The Program Office is also NASA's institutional mechanism for disseminating the results of its research and development activities. These results are published by NASA in the NASA STI Report Series, which includes the following report types:

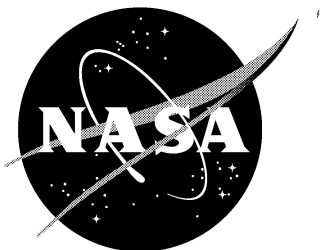
- **TECHNICAL PUBLICATION.** Reports of completed research or a major significant phase of research that present the results of NASA programs and include extensive data or theoretical analysis. Includes compilations of significant scientific and technical data and information deemed to be of continuing reference value. NASA counterpart of peer-reviewed formal professional papers, but having less stringent limitations on manuscript length and extent of graphic presentations.
- **TECHNICAL MEMORANDUM.** Scientific and technical findings that are preliminary or of specialized interest, e.g., quick release reports, working papers, and bibliographies that contain minimal annotation. Does not contain extensive analysis.
- **CONTRACTOR REPORT.** Scientific and technical findings by NASA-sponsored contractors and grantees.
- **CONFERENCE PUBLICATION.** Collected papers from scientific and technical conferences, symposia, seminars, or other meetings sponsored or co-sponsored by NASA.
- **SPECIAL PUBLICATION.** Scientific, technical, or historical information from NASA programs, projects, and missions, often concerned with subjects having substantial public interest.
- **TECHNICAL TRANSLATION.** English-language translations of foreign scientific and technical material pertinent to NASA's mission.

Specialized services that complement the STI Program Office's diverse offerings include creating custom thesauri, building customized databases, organizing and publishing research results . . . even providing videos.

For more information about the NASA STI Program Office, see the following:

- Access the NASA STI Program Home Page at <http://www.sti.nasa.gov>
- Email your question via the Internet to help@sti.nasa.gov
- Fax your question to the NASA STI Help Desk at (301) 621-0134
- Telephone the NASA STI Help Desk at (301) 621-0390
- Write to:
NASA STI Help Desk
NASA Center for AeroSpace Information
7121 Standard Drive
Hanover, MD 21076-1320

NASA/CR-2002-211430



Experiments With Fixed and Adaptive Herschel-Quincke Waveguides on the Pratt and Whitney JT15D Engine

*Jerome P. Smith and Ricardo A. Burdisso
Virginia Polytechnic Institute and State University
Blacksburg, Virginia*

National Aeronautics and
Space Administration

Langley Research Center
Hampton, Virginia 23681-2199

Prepared for Langley Research Center
under Grant NAG1-2137

March 2002

Available from:

NASA Center for AeroSpace Information (CASI)
7121 Standard Drive
Hanover, MD 21076-1320
(301) 621-0390

National Technical Information Service (NTIS)
5285 Port Royal Road
Springfield, VA 22161-2171
(703) 605-6000

TABLE OF CONTENT

TABLE OF CONTENT	1
ABSTRACT	3
1. INTRODUCTION	5
2. EXPERIMENTS WITH FIXED HQ TUBES	7
2.1 THE JT15D ENGINE AND TEST CELL	7
2.2 THE HQ INLET	7
2.3 MEASUREMENT FACILITIES.....	9
2.4 EXPERIMENTAL RESULTS	10
3. EXPERIMENTS WITH ADAPTIVE HQ TUBES ON THE JT15D ENGINE 14	
3.1 ADAPTIVE-FLAP HQ-TUBE SYSTEM	14
3.2 EXPERIMENTS USING THE ADAPTIVE-FLAP HQ-TUBE.....	18
3.3 ADAPTIVE-LENGTH HQ-TUBE SYSTEM	22
3.4 EXPERIMENTS USING THE ADAPTIVE-LENGTH HQ-TUBE.....	25
3.5 ADAPTIVE CONTROL SYSTEM.....	26
4. CONCLUSIONS	34
5. RECOMMENDATIONS FOR FUTURE RESEARCH	34
ACKNOWLEDGEMENTS	35
REFERENCES	35

ABSTRACT

This report presents the key results obtained by the Vibration and Acoustics Laboratories at Virginia Tech over the period from January 1999 to December 2000 on the project *“Investigation of an Adaptive Herschel-Quincke Tube Concept for the Reduction of Tonal and Broadband Noise From Turbofan Engines”* funded by NASA Langley Research Center. The Herschel-Quincke (HQ) tube concept is a developing technique that consists of installing circumferential arrays of HQ tubes around the inlet of a turbofan engine. This research is a continuation of previous efforts in which the HQ concept was preliminarily validated on the JT15D engine [1].

This final project report is organized in three separate reports. The research presented in these reports summarizes both analytical and experimental investigations of the HQ concept for reducing turbofan radiated inlet noise. The analytical part of the project involves two different three-dimensional modeling techniques to provide prediction and design guidelines for the application of the HQ-concept to turbofan engine inlets. First, an infinite-duct model was developed and used to provide insight into the attenuation mechanisms of the HQ systems and design strategies. Results from this analytical model show the effectiveness of the technique and are presented here. Second, the NASA-developed TBIEM3D code was modified to allow numerical modeling of HQ systems. This model allows for the investigation of the HQ system when combined within a passive liner. The experimental part of this work includes data for “fixed” HQ tubes on the JT15D engine with different inlet acoustic modal content than previously tested. Experimental results for fixed HQ tubes on a full-scale Honeywell TFE731-60 engine are also presented. Also included here is the first set of results of an experimental investigation into adaptive HQ configuration on the JT15D engine. The parameters of the HQ tubes are changed to optimize the attenuation as the engine speed is changed.

The first report presents the analytical modeling and simulation results. The second report describes the experimental results with both fixed and adaptive HQ-tubes on the JT15D engine. Finally, the third report describes the most important results with fixed tubes on the Honeywell TFE731-60 engine. The three parts of this final report are written such that each part is a complete and separate document that can be reviewed independently from the others.

1. INTRODUCTION

The Herschel-Quincke (HQ) tube concept consists of installing circumferential arrays of HQ tubes around the inlet and/or the by-pass duct of a turbofan engine. The application of HQ tubes to turbofan engine inlet noise is a developing technique originally pioneered at Virginia Tech. The research presented in this report is a continuation of previous efforts in which the HQ concept was preliminarily validated on the JT15D engine [1]. The accomplishments of the previous research efforts are summarized in an earlier report [1]. The main previous achievements include:

- Experimental results on the JT15D engine inlet demonstrated BPF tone power attenuation of up to 8 dB with fixed arrays of HQ tubes.
- The HQ tube concept also provides significant attenuation of the broadband component (~ 3 dB power reduction over 0-3200 Hz band.)
- An initial analytical model was developed to investigate the noise control mechanisms of the HQ tube concept and to guide in the design of experiments.

An overview of the tasks involved in this project is shown in Figure 1.1. The project has analytical and experimental components. The analytical part involves the development of two modeling tools for the HQ-tube concept applied to turbofan engine inlets. The experimental part consists of validating the approach in two engines, i.e. Pratt&Whitney JT15D and Honeywell TFE731-60 engines, for various HQ-tube configurations. The main objectives of this continuing research effort are:

- To further develop modeling techniques for the design, prediction, and optimization of the Herschel-Quincke (HQ) tube concept for application to turbofan engine noise.
- To experimentally investigate both fixed and adaptive HQ-systems for useful reduction of turbofan inlet noise with realistic components on a running turbofan engine.

The final report is organized in three parts devoted to the various components of the research endeavor. This report corresponds to *Part II*, which describes the experimental work performed on the Pratt & Whitney JT15D engine at Virginia Tech. Section 2 of the report presents tests using fixed HQ-tubes on the JT15D without the upstream rods used in previous experiments [1]. Removing the rods results in a different set of dominant modes in the inlet. Section 3 contains the first set of results using adaptive HQ tubes on the JT15D engine. Two adaptation mechanisms are described and tested on the engine. A control system was also developed to adjust the parameter of the HQ-tubes to maximize the attenuation of the BPF tone as the engine speed was changed.

ANALYTICAL WORK

VPI Infinite Duct Model

- Extend model.
- Study tone and broadband control.
- Investigate noise control mechanisms.
- Optimization.
- Design experiments.

HQTBIEM3D Model

- Implement HQ-tube modeling to TBIEM3D
- Combined Liner-HQ system.
- Study forward and aft. radiation.
- System optimization.
- Modeling of high-bypass engines.

EXPERIMENTAL WORK

Engine Experiments Fixed Tubes

- JT15D engine 1 and 2 arrays.
 - $m=1$ and $\mu=0,1,2,3$
 - $m=5$ and $\mu=0,1$
- Honeywell TFE731-60 Engine.
 - $m=2,-8,12$ and $\mu=0, \dots, 5$

Engine Experiments Adaptive Tubes

- Investigate tube adaptation mechanisms.
- Evaluate adaptive tubes on JT15D engine.
- Implement adaptive control system.
- Demonstrate adaptive HQ system on JT15D engine.

Figure 1.1: Overview of project tasks.

2. EXPERIMENTS WITH FIXED HQ TUBES

This section presents the experimental setup and results for the HQ concept with fixed tubes on the inlet noise radiated by the JT15D turbofan engine at Virginia Tech. The fixed-tube experimental research goals for this year were to demonstrate the HQ concept on the JT15D engine without the exciter rods installed upstream of the fan. Removing these rods resulted in a different acoustic inlet modal configuration than previously tested with the rods.

2.1 THE JT15D ENGINE AND TEST CELL

The engine used for this research project is a Pratt and Whitney JT15D turbofan engine. This engine has been used in previous NASA studies and has been used extensively for research in active noise control methods applied to turbofan engines [2-5]. It is a twin spool turbofan engine with a full length bypass duct and a maximum bypass ratio of 2.7. There is a single-stage axial flow fan with 28 blades and a centrifugal high pressure compressor with 16 full vanes and 16 splitter vanes. There are no inlet vanes and the diameter at the fan stage location is 0.53 m (20.8 in). Experimental results were obtained by operating the engine at various speeds near the idle condition which corresponds to a fan speed range of approximately 5250 rpm, yielding a blade passage frequency (BPF) ranging from 2225-2520 Hz. Near this condition, the inlet intake flow speed is about 42.5 m/s which yields a Mach number of $M=0.12$. The engine is equipped with an inlet inflow control device (ICD) constructed at Virginia Tech from a NASA design [6]. The purpose of the ICD is to minimize the spurious effects of ground testing on acoustic measurements by breaking up incoming vortices. The maximum diameter of the ICD is 2.1 times the engine inlet diameter.

In previous tests, in order to enhance the tonal nature of the inlet radiated sound and to excite the $m=1$ mode to dominance, a set of 27 exciter rods were mounted upstream of the fan stage [1]. In the tests presented here, the rods were removed to provide a different modal configuration.

The engine test cell consists of two chambers, with the forward section consisting of a semi-anechoic chamber to simulate free field conditions. One wall of the semi-anechoic chamber is open to the atmosphere for engine intake air.

2.2 THE HQ INLET

In order to facilitate the rapid installation and removal of the HQ tubes on the engine inlet, a compact inlet section was constructed, which could be configured as either a rigid wall or with HQ elements. The inlet consists of a perforated mesh cylindrical skeleton, supported at each end by two circular plate rings and in the middle by four rectangular beams located geometrically 90° apart. The HQ elements could then be mounted behind the perforated mesh cylinder. A hard-wall inlet could be implemented by mounting sections of a hard, rigid material behind the mesh skeleton. The hard material used here

was 6.3 mm (0.25 in) thick ABS plastic. The inner diameter of the inlet was 0.53 m (20.8 in) in order to match the diameter of the engine at the fan stage where the inlet was to be mounted. The length of the inlet in the axial direction was 0.46 m (18 in), including the two 6 mm (0.25 in) thick plate rings at each end of the inlet to allow attachment of the inlet to the engine at one end and the attachment of the ICD to the inlet at the other. In these experiments, one or two arrays of HQ tubes are mounted circumferentially around the cylindrical perforated mesh inlet of the turbofan jet engine. The surface area of the inlet section where the tubes were not attached was configured as a rigid wall. The inlet has a length/diameter ratio $L/D \approx 1$, which is typical of turbofan engines. All of the tubes are axially-oriented (i.e., parallel to the engine axis) as shown in the configuration schematic in Figure 2.1. Figures 2.2(a) and 2.2(b) show pictures of the engine inlet configured as a rigid wall and with two arrays of HQ tubes, respectively. In Figure 2.2(b) the bottom panel is left off so that the mesh screen cylinder is visible.

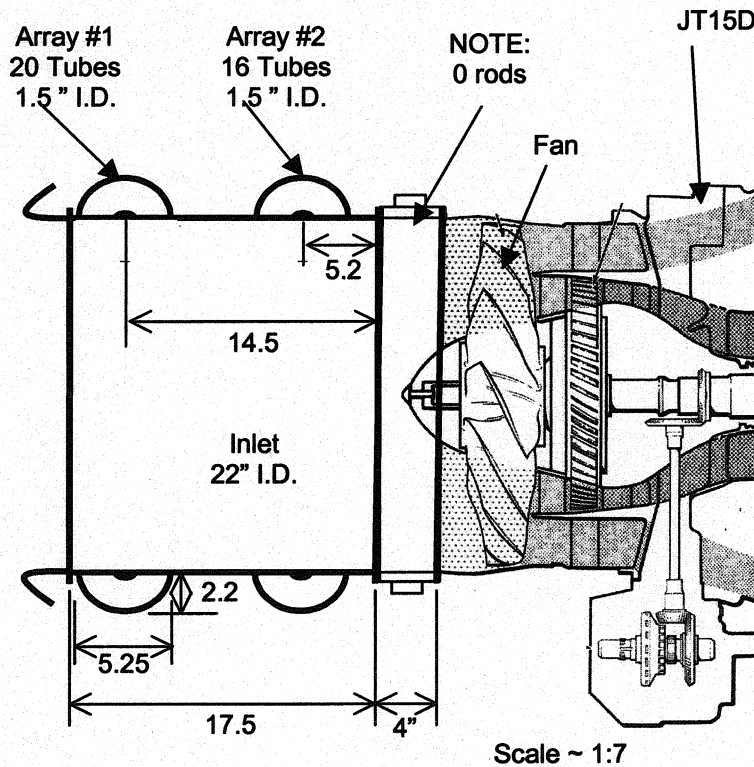
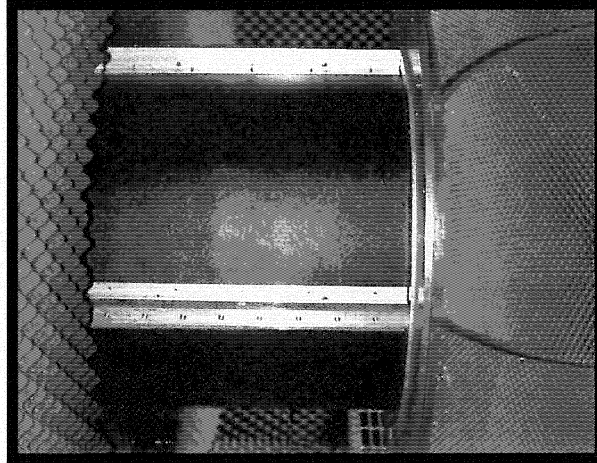


Figure 2.1: Schematic of experimental configuration for fixed HQ tubes on the JT15D without rods.

The tubes and panels were both constructed of black ABS plastic. The tube dimensions were designed so that their second resonance occurs in the vicinity of the first engine BPF tone near 2320 Hz , and each have a diameter of 3.8 cm (1.5 in) and an effective bypass length of 11.2 cm (4.4 in). The case shown in Figure 2.1 is for the first array (away from the fan) containing a total of 20 tubes, and the second array (closest to the engine) containing 32 tubes. However, the second array can also be configured with 16 tubes by simply blocking half of them. When both arrays were implemented

simultaneously, the tubes occupied less than 8.1% of the total surface area of the inlet. The adaptive HQ tube arrays were also mounted in a similar fashion. The mechanisms and dimensions of the adaptive HQ tubes will be presented in the experimental results section.

(a)



(b)

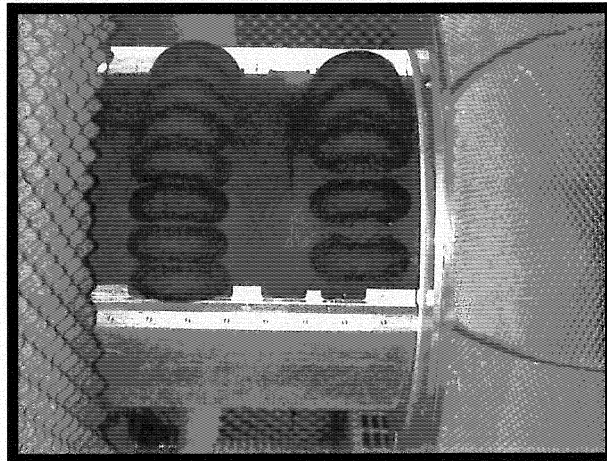


Figure 2.2: Pictures of experimental configuration for (a) hard wall, (b) fixed HQ-tubes (2 arrays of 20 and 32 tubes) on the JT15D without rods.

2.3 MEASUREMENT FACILITIES

The acoustic field of the JT15D engine was monitored with an array of 31 farfield microphones positioned in the horizontal plane passing through the centerline of the engine. The microphones were spaced along an arc of radius 1.6 m (63 in) at 6° increments to obtain the acoustic directivity from -90° to 90° in the horizontal plane, (where 0° is along the engine axis). These microphones were used to evaluate the effects of the HQ tubes on the noise radiated by the engine.

2.4 EXPERIMENTAL RESULTS

Presented here are the key experimental results obtained with one and two arrays of Herschel-Quincke (HQ) tubes installed on the JT15D engine inlet, with the engine configured without excitation rods. All previous tests with the HQ tubes were performed with 27 rods located upstream of the fan [1]. These tests performed without the rods show the effect of the HQ tubes for the inlet with a different modal configuration. Both broadband and tonal data were obtained for a hard-walled inlet and for the inlet configured with one and two arrays of HQ tubes. Figure 2.1 shows a schematic of the engine configuration with both arrays of HQ tubes. When testing a single array, only Array 1 was used which contained 20 tubes. When implementing two arrays, Array 2 was added which contained 16 HQ tubes. As in previous tests, all tubes were identical and designed for their second resonance to occur near the BPF of 2320 Hz. The engine speed was varied to obtain data at several different BPFs ranging from 2260 to 2430 Hz.

The cut-on frequencies for the excited modes in the JT15D inlet with and without the 27 rods installed, respectively, are shown in Table 2.1. For the case with 27 rods, the 28 fan blades interact with the 27 rods to excite to dominance the $m=1$ circumferential mode. As shown in the table for the case with 27 rods, there are three radial modes cut-on below 2381 Hz, and the fourth radial mode cuts on above that frequency. For the case without rods, the only interactions that exist are between the fan blades and the stator vanes present in the engine. There are 66 stator vanes in the bypass region and 33 stator vanes on the core. The 28 fan blades interact with the 66 bypass stator vanes to excite the $m=28$ circumferential modes at BPF. However, all modes with circumferential order $m=28$ are cut-off below a BPF of about 6200 Hz, and thus these are evanescent modes, i.e. fan-bypass stator interaction is cut-off at the running speeds tested here. The 28 fan blades also interact with the 33 core vanes to excite $m=5$ modes at BPF. As shown in the table for the case with 0 rods, two radial modes with circumferential order $m=5$ are cut on above 2162 Hz. Thus, for the range of running speeds tested here without the rods, there appear to be two modes cut-on, the (5,0) and (5,1). Note that the interaction of the fan with the stators also takes place when the rods are installed, but the excitation of the $m=1$ modes due to the rods is significantly stronger than the excitation of the $m=5$ modes due to the core stators.

Table 2.1: Cut-off frequencies of JT15D Inlet Modes.

27 Exciter Rod		0 Exciter Rods	
Mode	Cut-off Freq. [Hz]	Mode	Cut-off Freq. [Hz]
(1,0)	374	(5,0)	1306
(1,1)	1084	(5,1)	2162
(1,2)	1737	(5,2)	2846
(1,3)	2381		
(1,4)	3021		

The acoustic power at the BPF tone was determined for the total sector (0° to 90°) and the sector toward the sidelines from 50° to 90° for the hard-walled inlet and the inlet

with one and two arrays of HQ tubes. Figure 2.3(a) shows the BPF tone power reduction over the 0° to 90° sector for the case without rods for various BPF tone frequencies tested. For the sake of comparison, Figure 2.3(b) shows the BPF power reduction for the same inlet configurations with the rods installed. It should be noted that the power of the BPF tone for the hard-walled inlet was about 15 dB higher with the rods installed, as it will be shown later. For the engine without rods, the HQ tubes show good reduction of the BPF tone power over the frequency range tested. The addition of the second array results in an average increase of approximately 2 dB in the achieved reduction of the BPF tone power. The most reduction was achieved with two arrays at a BPF of 2264 Hz (the lowest frequency on the range tested) with a total BPF power reduction of 4.9 dB. The power reduction over the sector from 50° to 90° was 5.4 dB. From the data, it appears as though the optimal BPF for both one and two HQ tube arrays may be below the lowest frequency in the range tested here.

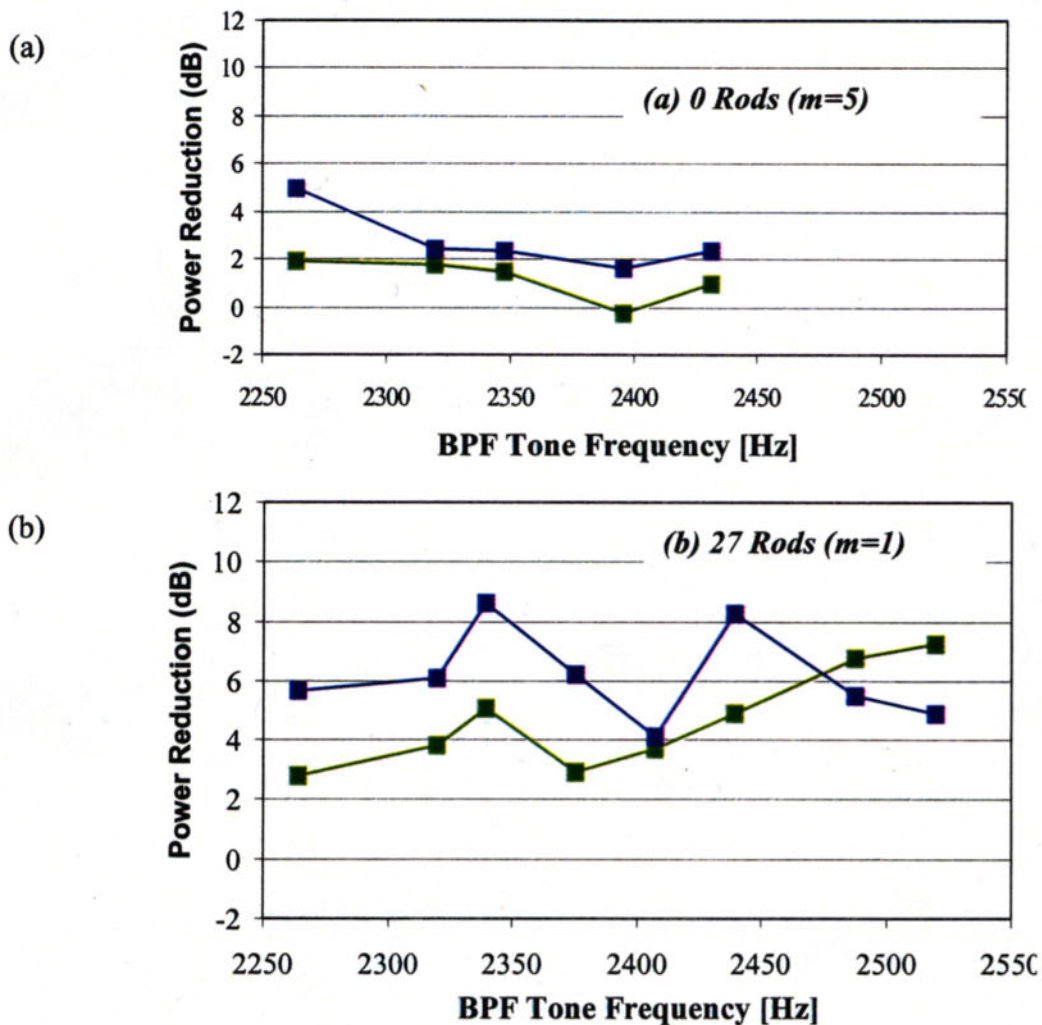


Figure 2.3: Total power reduction at BPF tone over 0° to 90° sector with fixed HQ tubes for (a) 0 exciter rods and (b) 27 exciter rods.

The broadband power spectra for the 0° to 90° sector without and with rods installed are shown in Figures 2.4(a) and 4(b), respectively. These figures show that the presence of the rods increased the BPF tone power ~ 15 dB while the broadband components did not change appreciably. The broadband content shows reduction over most of the frequency range with the most significant levels of reduction in the vicinity of the first (~ 1200 Hz) and second (~ 2400 Hz) resonances of the tubes for both with and without rods cases. However, the broadband attenuation is better for the case with rods. In figure 2.4a, broadband power reductions exceed 6 dB with 2 arrays of HQ tubes at frequencies in the vicinity of the first resonance. The overall broadband power reduction over the total sector (excluding the tone) was 1.7 dB with 2 arrays and 0.9 dB with one array. These overall reductions would only increase by about 0.1 dB if the reduction at the tone was included in the calculation of the overall reduction. Thus, the tone reduction does not contribute significantly to the overall reduction when the rods are removed. The overall broadband power reduction over the sector from 50° to 90° (excluding the tone) was 2.2 dB with 2 arrays and 1.3 dB with one array, and again these overall reductions would only increase by 0.1 dB if the reduction at the tone was included in the overall reduction.

It is evident from the experimental data that the HQ tube concept is effective for reducing the inlet noise radiated from the JT15D engine without the presence of exciter rods. Without the rods, two radial modes with circumferential order $m=5$ are excited. The HQ concept results in both tonal and broadband noise reduction for this modal configuration. Two HQ arrays yielded a 4.9 dB reduction in the BPF tone power and an overall broadband reduction of 1.7 dB. As in previous experiments with the rods, two arrays of tubes are shown to increase the reduction achieved at both the tone and in the broadband levels.

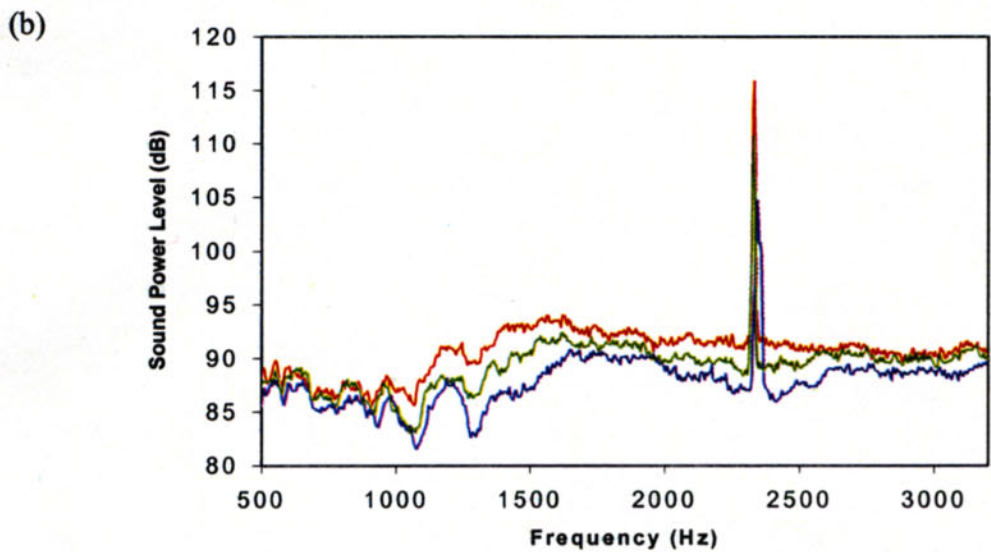
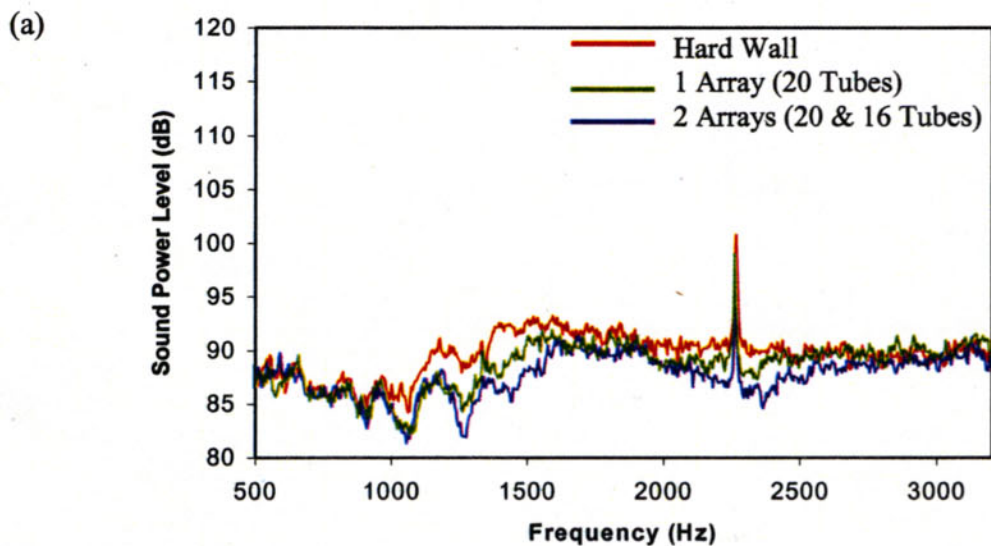


Figure 2.4: Broadband power reduction with fixed HQ tubes (a) no rods (b) 27 rods.

3. EXPERIMENTS WITH ADAPTIVE HQ TUBES ON THE JT15D ENGINE

In this section, the setup and results of the preliminary investigation into the potential of using adaptive HQ tubes is presented. It is clear that although the tubes are very effective over a range of BPFs, there is an optimal BPF at which the best attenuation occurs. This implies that in order to optimize the attenuation effect of the tubes over a wide range of BPF tones, the tubes should be adapted to “track” the BPF as it changes. The optimal attenuation frequencies depend on the geometry of the HQ tubes. Thus, the tube properties can be adjusted in real time for optimal tube performance as the BPF tone changes with engine conditions. The properties of the tube such as the length, cross-sectional area, and so forth can be modified in real time to provide optimal reduction of the inlet fan tone noise over the desired sectors in the far-field. The adaptation of the tube dynamics can be implemented with a control scheme (i.e. feedback, feedforward, etc.) as depicted in the schematic in Figure 3.1. The error signal used by the controller will be obtained from either far-field or inlet mounted microphones. The signals from these microphones will be processed to generate a signal proportional to the acoustic power radiated by the fan. The controller will then adjust the tube properties to minimize the observed radiated power. Since the optimal frequency of reduction for a set of HQ tubes is related to the HQ tube resonant frequencies, an effective actuation mechanism is expected to be one that effectively and linearly changes the resonant frequencies of the HQ tube. It is important to remark that the purpose here is not to develop a practical adaptation mechanism but rather investigate the potential of adaptive HQ-tube systems.

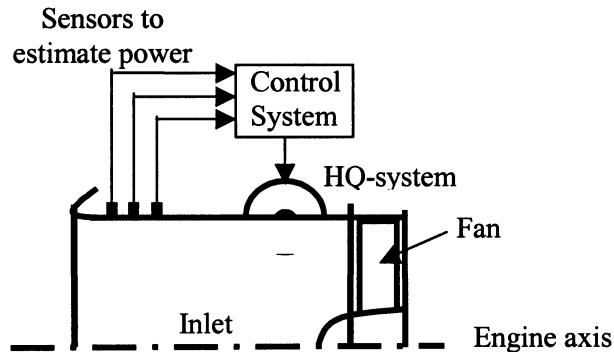


Figure 3.1: Schematic of adaptive HQ tube system applied to turbofan engine inlet.

3.1 ADAPTIVE-FLAP HQ-TUBE SYSTEM

Figure 3.2 shows one of the adaptation mechanisms proposed and preliminarily investigated. An internal “throttle-plate” flap is introduced into the tube and changes the resonant frequencies of the HQ tube when the angle α of the flap changes. This mechanism is relatively easy to mechanize and requires no change in the external space required by the HQ tubes. The first step was to characterize the actuation mechanism in terms of its effect on changing the resonant frequencies of the HQ tubes. To characterize the adaptive-flap mechanism, a speaker was mounted on one end of the tube (with the effects of the perforated screen included) and a microphone positioned close to the other

end, which was left open. The speaker was driven with white-noise and the transfer function between the speaker input and the microphone was obtained for various flap angles. Note that this test configuration does not accurately determine the absolute frequency values of the open-open tube resonances due to the placement of the speaker, but it provides a simple test in which the actuation mechanism can be evaluated in terms of the change in the resonant frequencies.

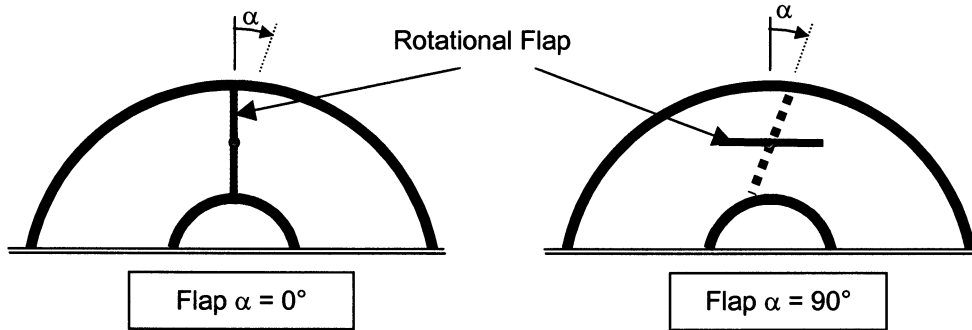


Figure 3.2: Schematic showing adaptive-flap HQ tube mechanism

Figure 3.3 is a plot of the frequency response between the speaker and the microphone for various values of the flap angle α . The first and second resonance frequencies of the HQ tube with the flap are indicated by the arrows. Note that the other two peaks in the FRF near 600 Hz and 1300 Hz are speaker effects as they were determined by testing the speaker alone. It is clear from this plot that the second resonance frequency of the tube increases with the flap angle α . However, it is also clear that the shape of the response around the resonant frequency changes with the flap angle as well. It is believed that the most desirable resonance for optimal reduction with the HQ tube is a sharp, well-defined single peak, the best example being the response curve for $\alpha = 30^\circ$. Thus, it appears that desirable resonant behavior will occur when the flap angle is near $\alpha = 30^\circ$ and that the response may have some non-linear effects as α gets too large or too small. For the flap at $\alpha = 0^\circ$, the HQ-tube is theoretically transformed into two quarter-wave tubes of half the length of the HQ-tube. Thus, the first resonance frequency of the quarter-wave tube should be half the second resonance frequency of the HQ-tube. However, it is important to note that the flap did not perfectly sealed the tube to form two quarter-wave tubes, and thus there were leaks between the flap and the inside wall of the tube.

It should also be noted that changing the flap angle does not significantly change the first HQ resonant frequency near 1000 Hz. This is due to the fact that the flap is located at the center of the HQ tube, where for the odd resonant frequencies there is a pressure anti-node (i.e. pressure is maximum and the particle is zero). Because the flap leads to changes in the tube cross-sectional area, it cannot affect the kinetic energy of the odd modes. On the other hand because the even modes have a pressure node at the tube's center (i.e. maximum particle velocity), the kinetic energy increases as the flap reduces the cross sectional area and the resonance frequency drops. The potential of affecting only even modes could be a desirable approach. For example, if the 3rd tube resonance is

targeted to control the BPF tone at a high engine power setting, adjusting the 2nd resonance of the tube to be optimum at controlling the BPF tone at a lower engine power setting may be required. Another potential application is if the optimal frequencies of reduction for the first HQ resonance wish to be kept fixed (e.g., for low-frequency broadband noise), while only the second resonance corresponding to the changing BPF is to be changed.

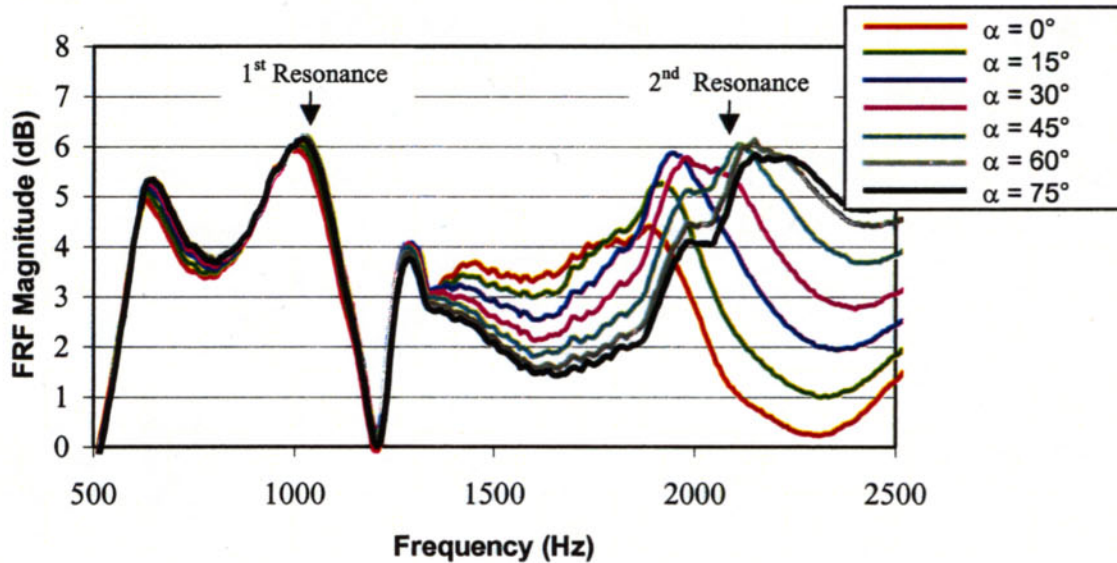


Figure 3.3: FRF showing adaptive-flap HQ tube resonant frequency change with flap angle.

Twenty tubes were constructed with the adaptive flap mechanism, installed on the JT15D, and the attenuation effects evaluated at different BPF frequencies for flap angles ranging from 0° (completely shut) to 90° (open or horizontal.) A stepper-motor system was implemented to control the flap angles with a 2° resolution. Figure 3.4 shows a schematic of the inlet as configured with the adaptive HQ tube array. Also installed on the inlet with the adaptive array is an additional fixed array containing 16 tubes. Thus the effects of the adaptive array were tested alone and in addition to the single fixed array. Figure 3.5 contains a picture showing the adaptive array inlet mounted on the JT15D and a close-up of the adaptation mechanism with a stepper motor. A total of four stepper motors were used, with one motor mounted on each of the four quarter-panels to control the flaps on their respective panels. All four motors were controlled by a single stepper-motor controller which supplied the same actuation signal to each motor. The motors were connected to the tube flap axes by a direct-drive chain as shown in the picture. The rotating flap axis of each tube on the same panel were connected with universal joints so that all of the flaps on the same panel moved together.

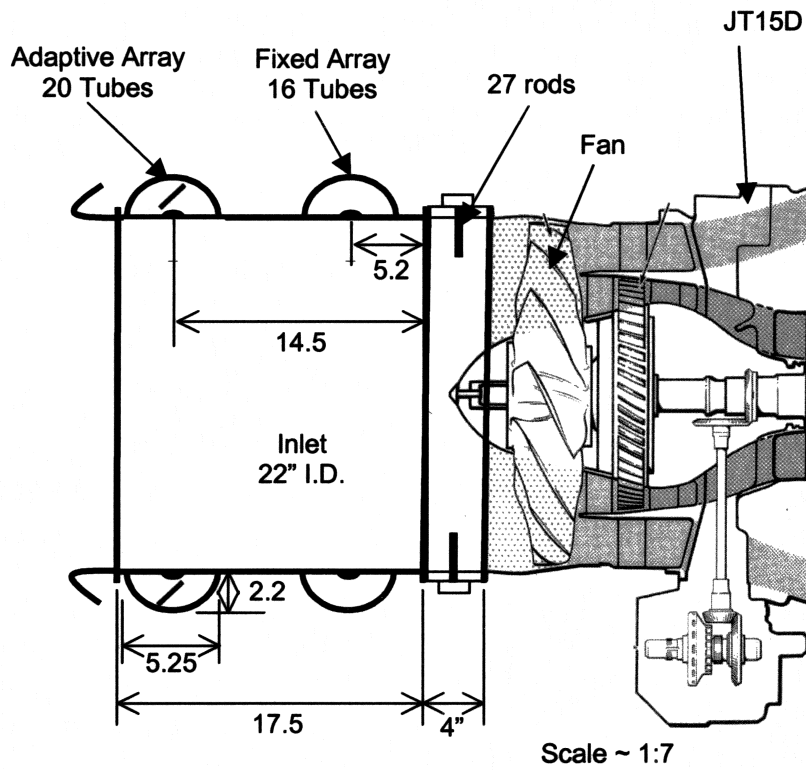


Figure 3.4: Schematic of experimental configuration for adaptive-flap HQ tubes on the JT15D.

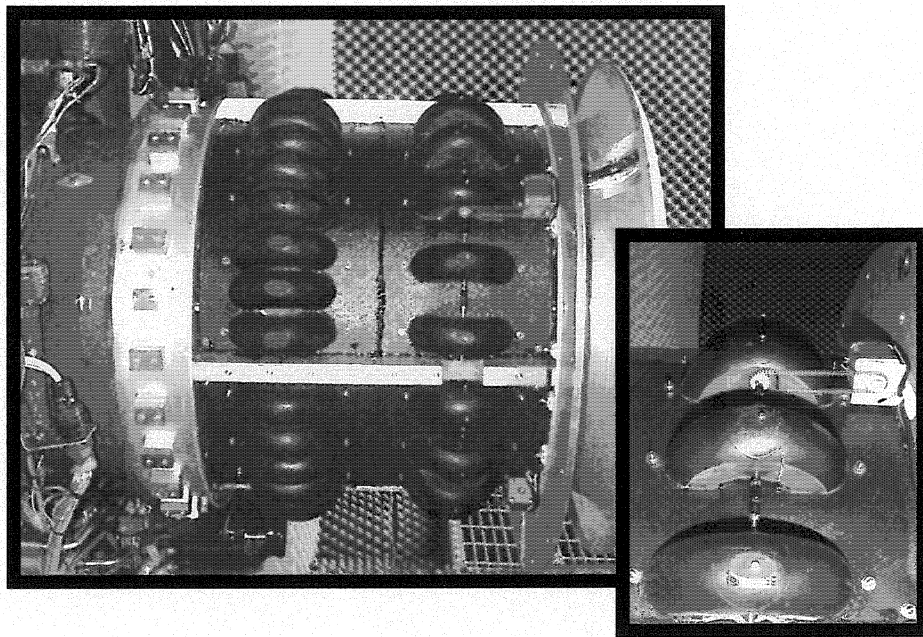


Figure 3.5: Pictures showing experimental configuration for adaptive-flap HQ tubes on the JT15D.

3.2 EXPERIMENTS USING THE ADAPTIVE-FLAP HQ-TUBE

The adaptive-flap HQ-tube system shown in figure 3.5 was tested on the JT15D engine. Figure 3.6 shows the total BPF power reduction over the range of flap angles for three different BPF frequencies with the single adaptive array. Starting with the BPF of 2360 Hz (the blue curve) a total of 6 dB reduction is achieved with an optimal flap angle of $\alpha=30^\circ$. As seen by moving downward to the magenta curve, if the engine speed were increased to a BPF of 2560 Hz, the BPF reduction would drop to about 3.2 dB. But, as predicted by the flap characterization, opening the flap angle to $\alpha=50^\circ$ results in an increase of the BPF reduction to about 5 dB at the higher BPF. Now, starting again at the blue curve with $\alpha=30^\circ$, if the engine speed were to decrease to result in a BPF of 2280 Hz, the reduction would drop to about 4 dB. The earlier characterization of the flap mechanism would imply that the flap angle needs to be additionally closed to result in optimal reduction for a lower BPF, but as seen in the figure, closing the flap does not result in an increase in the BPF reduction. The best reduction achieved at a BPF of 2280 Hz was about 4.8 dB, with the flap angle completely closed. Thus, it appears that the flap mechanism does not perform well for the extremes flap positions, i.e. $\alpha\sim 0^\circ$ and $\alpha\sim 90^\circ$.

The effects of the adaptive-flap HQ array on the BPF power reduction with the addition of the second fixed array for four different BPFs are shown in Figure 3.7. In a similar fashion as in the previous figure, starting at the BPF of 2340 Hz (the dark blue line) at the optimal flap angle of $\alpha=30^\circ$, the BPF reduction is seen to be almost 8 dB. If the BPF were to change up to 2520 Hz, the reduction would drop to only 4.5 dB. If the flap angles were now opened to $\alpha=50^\circ$, the reduction would increase to about 7.3 dB. Unfortunately, no flap angles existed for regaining such a significant amount of BPF power reduction when changing the engine speed above and below this BPF range.

It should be noted that at several BPF test frequencies, the effect of the flap angle on the total BPF power reduction did not follow an observable trend with the change in flap angle α . The initial characterization testing of the adaptive flaps did show the potential of this particular adaptation concept for increasing the reduction obtained with the HQ tubes over a range of running speeds. However, the range of frequencies obtainable with the flap mechanism was somewhat limited.

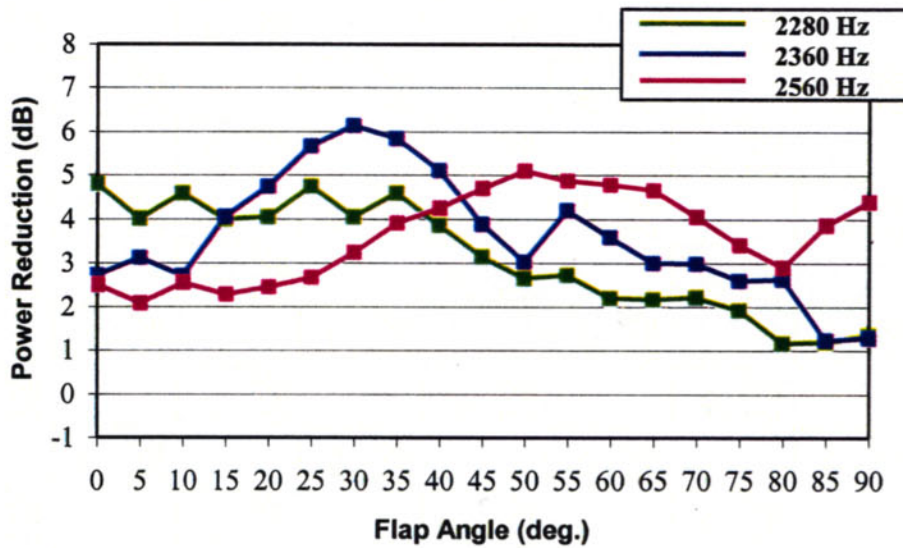


Figure 3.6: Power reduction at the BPF tone versus flap angle for several BPFs using the single adaptive-flap array.

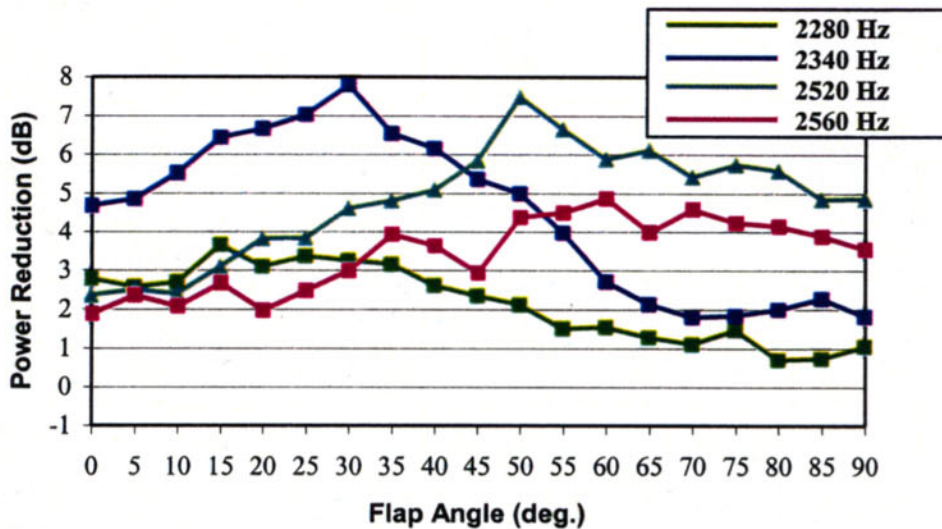


Figure 3.7: Power reduction at the BPF tone versus flap angle for several BPFs using the single adaptive-flap array in combination with the fixed array.

The effect of the adaptive flap on the inlet radiated broadband noise was also investigated. Figure 3.8 shows the total A-weighted power spectra from 0 to 3200 Hz for the hard-wall inlet and for the single adaptive-flap HQ array with flap angles of $\alpha=50^\circ$ and $\alpha=80^\circ$. Figure 3.9 contains the same plot for the case with the single adaptive-flap array and the fixed array with 16 tubes both on the inlet. It is evident from these plots that the flap angle clearly has an effect on the frequency of optimal reduction due to the second resonance of the tubes (near 2400 Hz), while the optimal frequency of reduction

for the first resonance (near 1300 Hz) remains essentially unchanged. It appears that the optimal frequency of reduction due to the second resonance is near 2000 Hz with the flap angle at $\alpha=50^\circ$, and up near 2600 Hz with $\alpha=80^\circ$ for both the single adaptive-flap array alone and the single adaptive-flap array together with the fixed HQ array. Also clear is the significant increase in the overall reduction with the two arrays of tubes as compared to the single adaptive array alone.

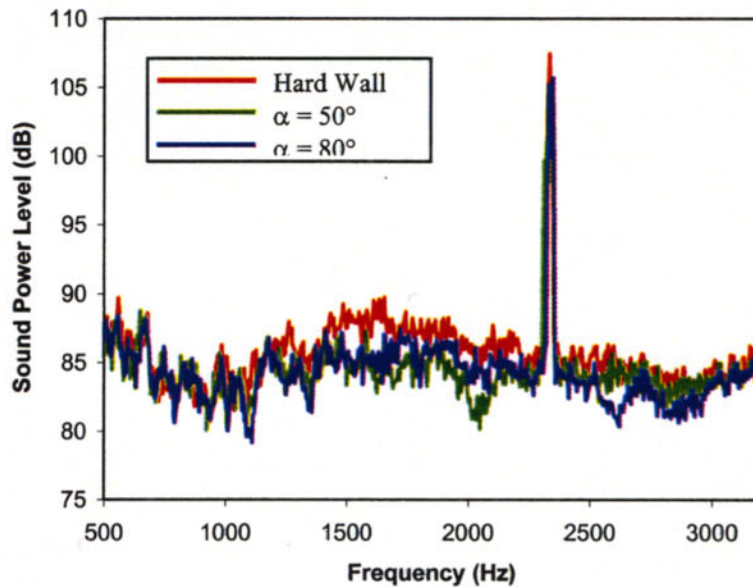


Figure 3.8:Total A-weighted power spectra using the single adaptive-flap array.

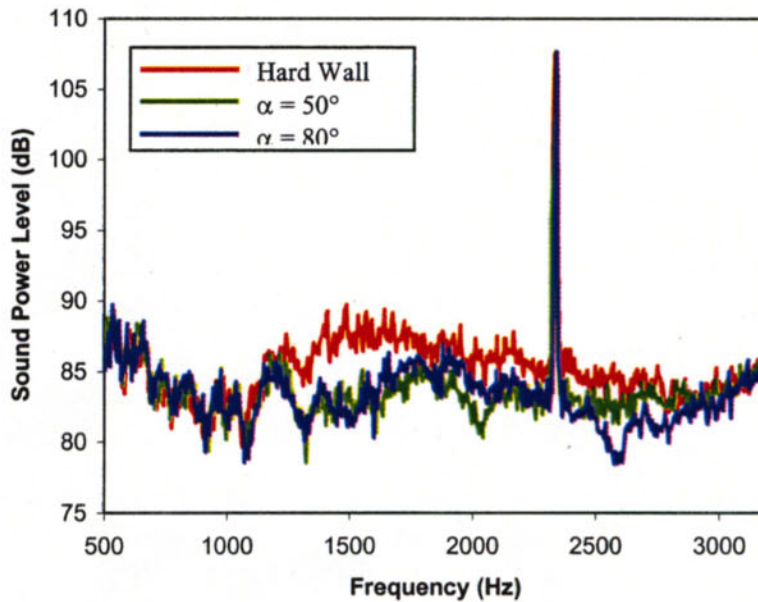


Figure 3.9:Total A-weighted power spectra using the single adaptive-flap array in combination with the fixed array.

In general, the optimal frequency of reduction in the broadband noise content was seen to increase with increasing flap angle, as predicted with the characterization resonance tests. This effect is more obvious in the plots of Figure 3.10 (a) and (b) which show the total broadband power reduction versus frequency and flap angle α , for the single array of 20 adaptive tubes and the two-array case. The first optimal frequency of reduction appears to be unaffected by the change in flap angle. However, the frequency variation of the second optimal frequency of reduction can be seen as a near “ \sim ” shape, i.e., does not change significantly with flap angle at the low and high angles (from $\alpha=0^\circ$ to $\alpha=20^\circ$ and from $\alpha=60^\circ$ to $\alpha=90^\circ$), but changes almost linearly with flap angles between $\alpha=25^\circ$ and $\alpha=55^\circ$. Thus, it seems that the flap angle results in a controllable effect only over a relatively small flap angle range, corresponding to a relatively small frequency range. It is noted here that the absolute level of broadband noise reduction did not change significantly with the flap angle, as shown in Figures 3.11(a) and (b) showing the A-weighted broadband power reduction from 0 to 3200 Hz excluding the tone versus flap angle for the one and two array cases, respectively.

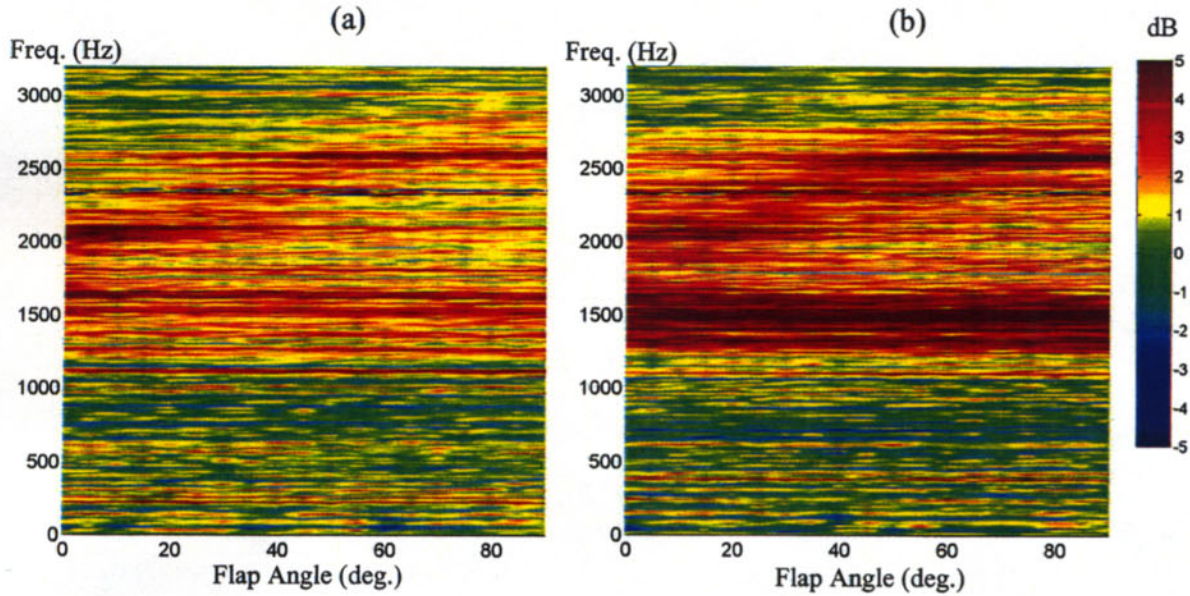


Figure 3.10:Total power reduction versus frequency and flap angle (a) single adaptive-flap array (b) single adaptive-flap array in combination with the fixed array.

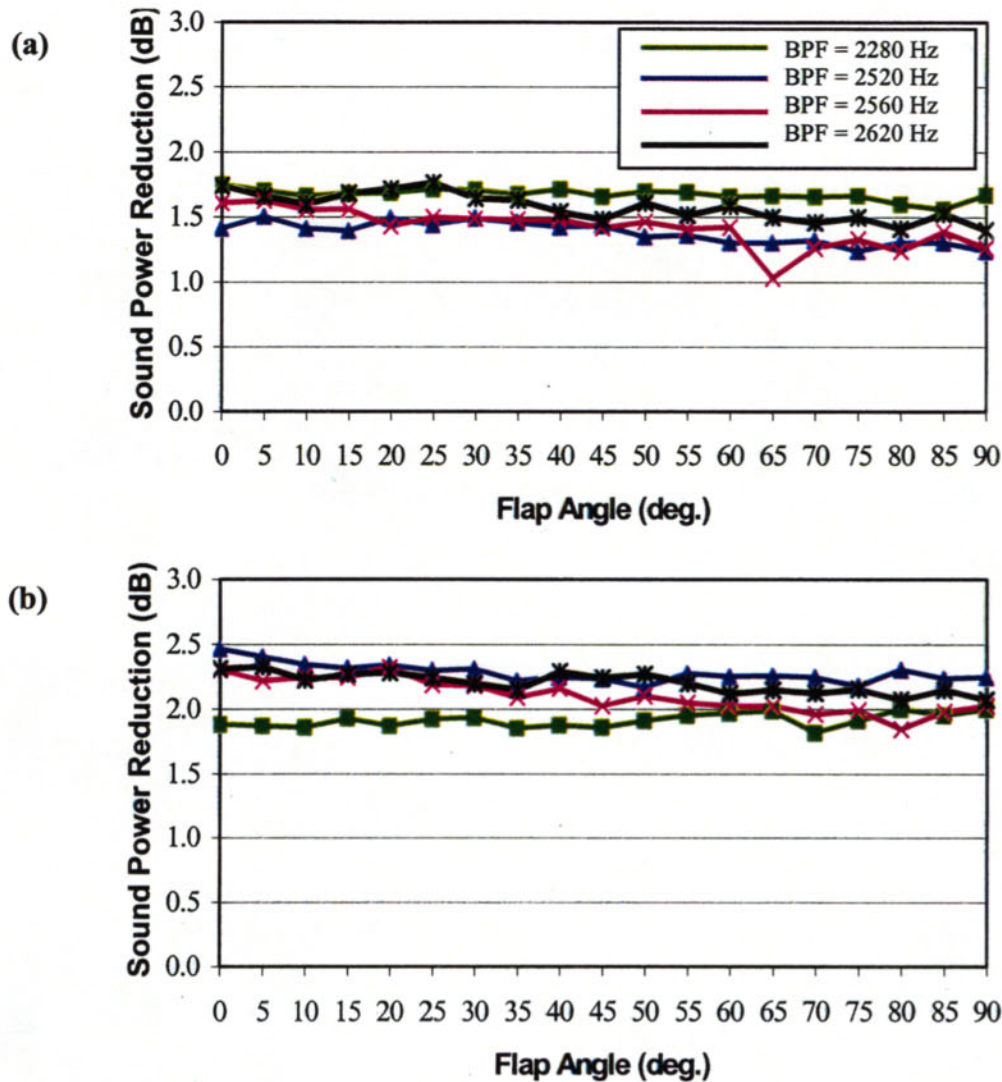


Figure 3.11:Total A-weighted broadband power reduction 0-3200 Hz (no tone) versus flap angle (a) single adaptive-flap array, (b) single adaptive-flap array in combination with the fixed array.

3.3 ADAPTIVE-LENGTH HQ-TUBE SYSTEM

Due to the drawbacks stated concerning the adaptive-flap HQ array adaptation technique, another adaptation approach involving changing the length of the tubes was investigated. It was expected that changing the tube length would provide a more linear adaptation mechanism. The first design of the adaptive-length mechanism is shown in Figure 3.12. Both tube ends are attached to the inlet through an expendable rubber section. The tube length is then controlled by the rotation of a screw into a nut fixed to the HQ-tube. A stepper motor then drives the screw. By turning the screw, the tube could be pulled up and down, allowing the effective length of the tube to change. Several mechanisms for changing the tube length were investigated; the method chosen was

based on ease of mechanization. The advantage of the adaptive length mechanism is that moving the tube a height “d” results in a change in the effective length equal to 2d. The second system consists of tubes of changeable length. The tube lengths range approximately from 11.5 to 13.3 cm.

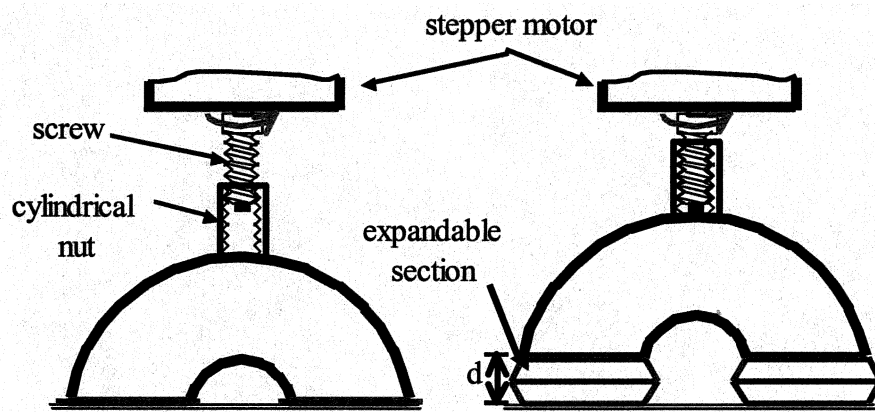


Figure 3.12: Schematic showing prototype for adaptive-length HQ tube mechanism.

The adaptive-length tube was characterized in the same manner as the adaptive-flap tube explained earlier, i.e., by placing a speaker at one end and a microphone at the other, and measuring the transfer function response with a white noise input to the speaker. The frequency responses showing the resonant frequency change for a variable change in length Δ are shown in Figure 3.13. Both the first and second resonances show clear, sharp resonant behavior and a linear change in resonant frequency as the length of the tube changes. Note that this data was obtained without the perforated screen, the presence of which will change the absolute values of the resonant frequencies. An approximate 14% change in the tube length resulted in a corresponding 14% change in the second resonant frequency, which changed from approximately 1700 Hz to 1450 Hz over the full range of motion of 15 mm. From these characterization results, it is expected that the adaptive length tube will work better than the adaptive-flap technique over a wide range of frequencies.

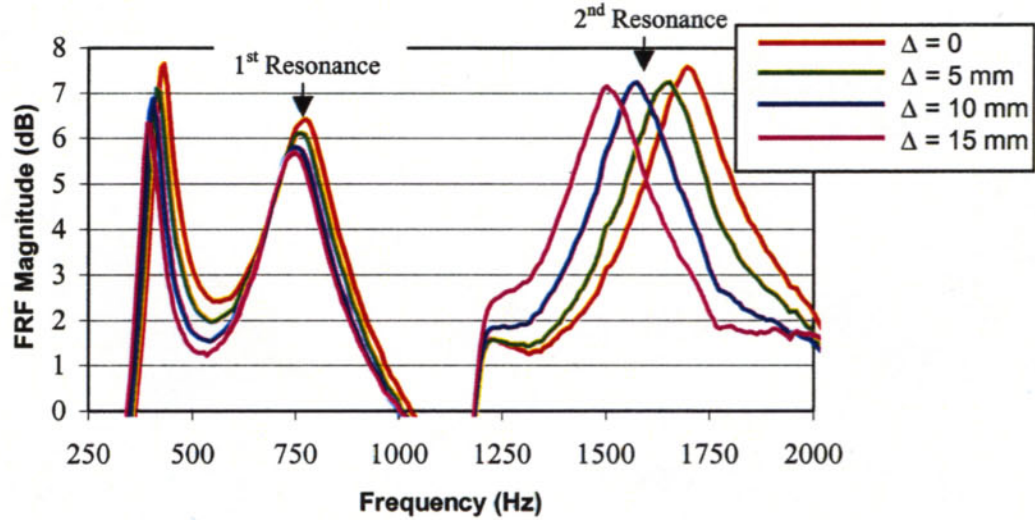


Figure 3.13: FRF showing adaptive-length HQ tube resonant frequency change with length parameter D.

Twenty tubes were constructed with the adaptive-length mechanism, installed on the JT15D. Each tube was adjusted by a separate stepper-motor driven with the same driver to obtain the same adjustment in all the tubes. Figure 3.14 contains a picture showing the adaptive array inlet mounted on the JT15D and a close-up of the adaptation mechanism with the stepper motors.

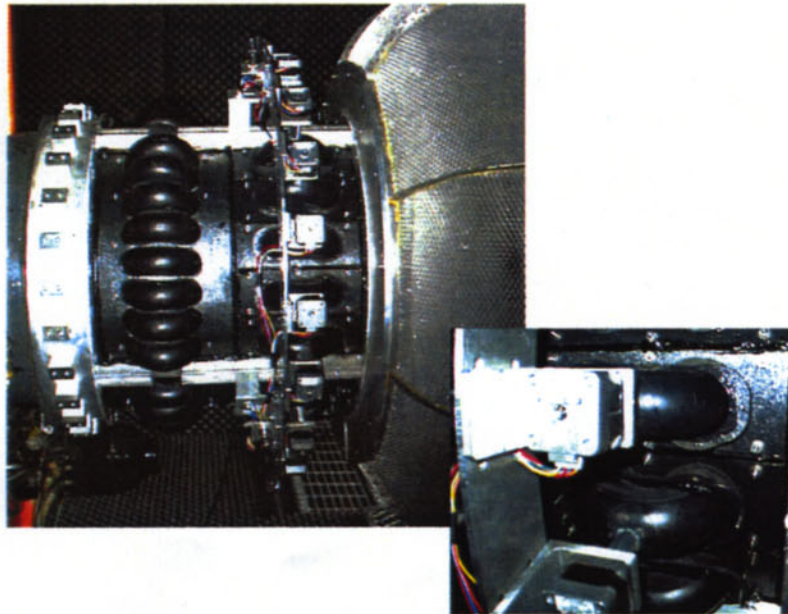


Figure 3.14: Pictures showing experimental configuration for adaptive-length HQ tubes on the JT15D.

3.4 EXPERIMENTS USING THE ADAPTIVE-LENGTH HQ-TUBE

The adaptive-length HQ-tube system shown in figure 3.14 was tested on the JT15D engine. As an illustrative example of the performance of the system, the sound power spectrum over the 0° to 90° sector for three different tube lengths at an engine speed yielding a BPF tone frequency of 2250 Hz was obtained. Figure 3.15a-c show the sound power spectrum for the hard wall condition and for the adaptive HQ-array at tube lengths of 11.5, 12.7, and 13.3 cm, respectively. It is clear that for the shortest tube length the optimum broadband attenuation at the first and second tube resonance occurs near 1200 and 2500 Hz, respectively. These frequencies of attenuation have shifted towards lower frequencies as the tube length is increased from 11.5 to 13.3 cm. In figure 3.15c, the frequencies of attenuation are now at approximately 1050 and 2000 Hz, respectively.

The BPF tone sound power reductions for the three cases shown in the figures 3.15a-c are 2.5, 5.1, and 5.2 dB, respectively. This result shows that the optimum length at the BPF tone of 2250 Hz is 13.3 cm. It is thus expected that the optimum length for higher BPF tone frequencies would be shorter. The effect of the tube length on the BPF tone power reduction will be demonstrated in the next section.

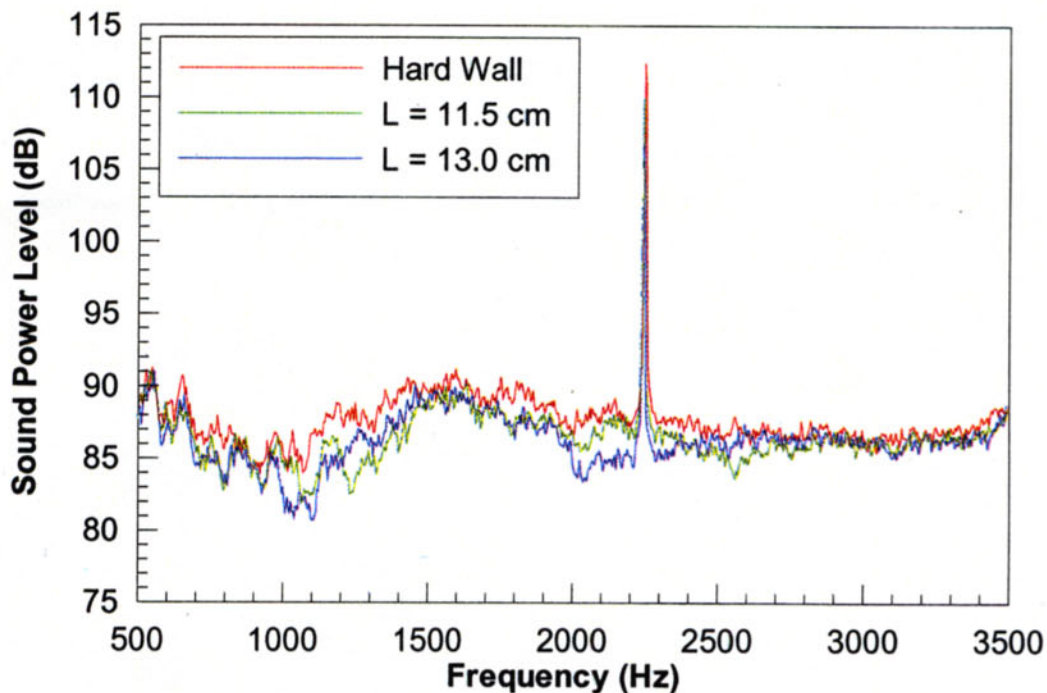


Figure 3.15: Sound power spectrum for adaptive-length HQ-tube for tube lengths of (a) 11.5, (b) 12.7, and (c) 13.3 cm.

The performance and effect on the frequencies of attenuation of the adaptive-length system is probably easiest to assess by plotting the broadband sound power reduction as a function of the tube length. This result will also be best to compare to the adaptive-flap mechanism. The sound power reduction as a function of tube length is plotted in figure 3.16a. It is very clear that by changing the length of the tubes, the frequency of power

attenuation around both the first and second tube resonance frequencies changes linearly. The dashed lines in the figure indicate the center frequencies of attenuation as a function of the tube length. The frequency changes for the first and second tube resonance are approximately 300 and 600 Hz, respectively. It is interesting to compare the performance of the two adaptation mechanisms. To this end, the broadband sound power for the “flap” mechanism is also plotted in figure 3.16 (same as figure 3.10a). It is evident that the “flap” mechanism changes only the second tube resonance frequency (over the angles $\alpha=25^\circ$ and $\alpha=55^\circ$) as compared to “length” mechanism that affects both the tube resonance frequencies.

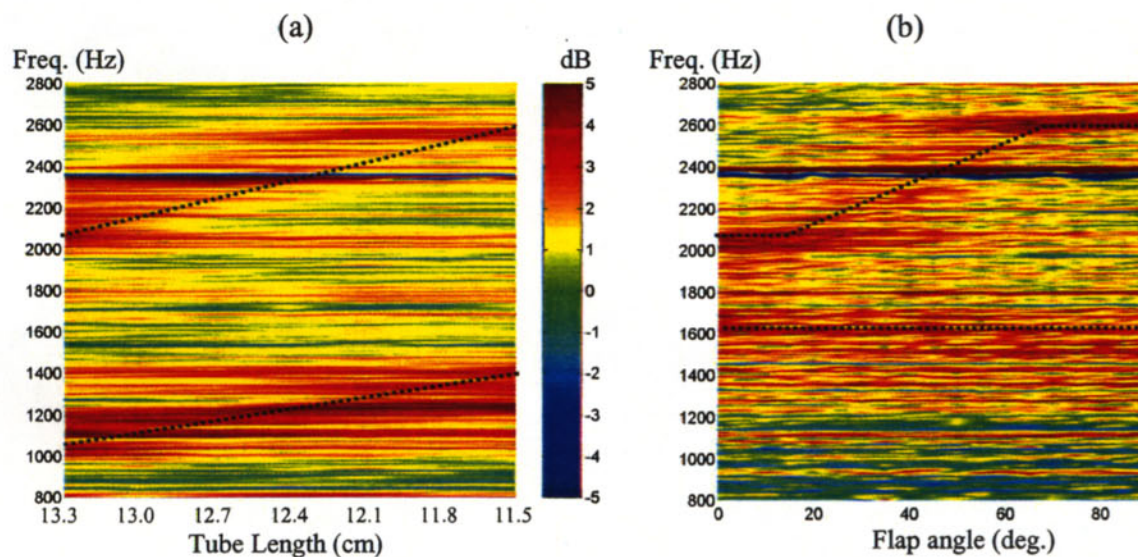


Figure 3.16: Broadband sound pressure level reduction using adaptive (a) length and (b) flap HQ-tube implementation.

3.5 ADAPTIVE CONTROL SYSTEM

Adaptive control can be used to adjust the tube parameter to optimize the attenuation of the BPF tone over a range of engine speeds. The term adaptive control is used here implying an “actuator” is implemented to adjust the HQ-system based on “error” information obtained from the sound radiation from the inlet. Though this is in fact an active system, it is not referred to as such to differentiate from previous active noise control approaches where a secondary sound field is introduced to destructively interfere with the fan noise. In other engineering fields, the adaptive system proposed here is commonly referred to as semi-active control.

The adaptation of the tube’s dynamics can be implemented with a control scheme as depicted in the schematic of figure 3.17. The error signal used by the controller is obtained from an array of microphones that can be mounted in the far-field (such as on the fuselage) or in the engine inlet. The signals from these microphones are input into high-Q band-pass filter (BPF extractor) to extract the signal at the BPF from the total

signal. Since the BPF changes with time, a proximity probe fixed on the inlet near the fan is used to track the BPF frequency. The BPF probe signal is used to adapt the center frequency of the band-pass filter. The filtered error signals are then a purely sinusoidal signal at the BPF. The RMS squared value of the BPF signal is then processed to generate a signal proportional to the total acoustic power radiated by the fan at the BPF over a sector on the far-field, i.e. sidelines. The sector where reduction is sought should be selected to have the maximum impact on the EPNLdB metric. An actuator will then adjust the tube properties to minimize the observed radiated power over the sector.

The adaptive-length mechanism was selected for the demonstration of the adaptive control system described above. The error microphones were positioned on the far-field at 18°, 30°, and 42° to minimize the BPF tone radiated over this sector. The microphone locations were selected because the inlet sound power is dominated by the flow of acoustic energy over the 15° to 50° sector.

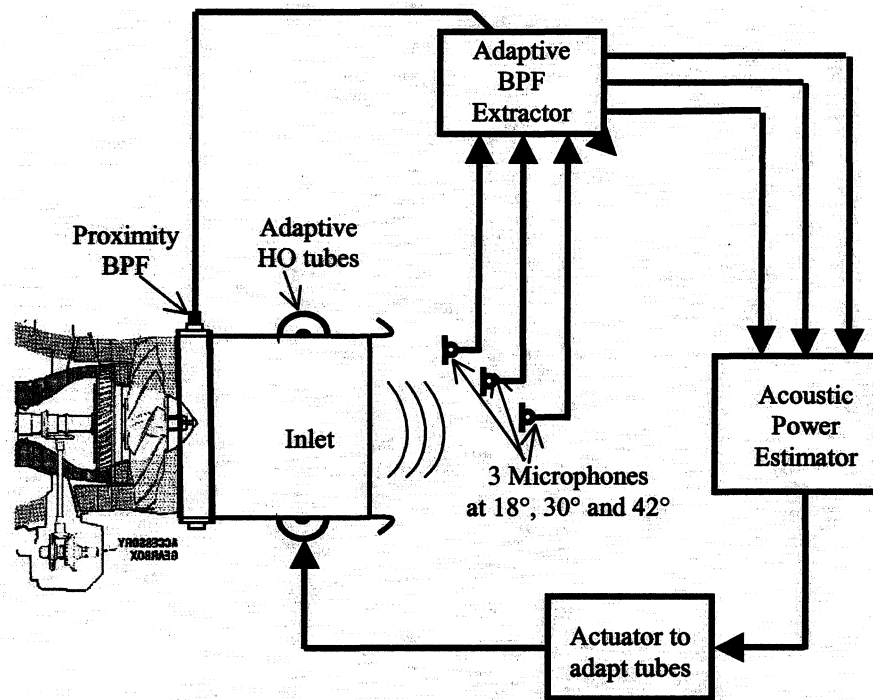


Figure 3.17: Schematic of adaptive control system.

The BPF extractor in figure 3.17 is needed to separate the BPF tone from the broadband component before the power of the BPF tone is estimated. The approach used here to separate the BPF tone is based on using switched-capacitor filter and phase-lock-loop circuits as shown in figure 3.18. The BPF tone is obtained from the total signal by using an analog, high-Q bandpass switched-capacitor filter whose center frequency is adjusted using an external clock signal. By changing the frequency of this clock signal,

the center frequency of the bandpass filter can be changed. To this end, a reference signal related to the BPF tone is used as an input into a Phase-Locked-Loop circuit which is designed to generate the clock signal. Taking the reference signal from the fan proximity probe transducer, the reference signal changes the clock signal and thus the filter center frequency as the engine speed varies. Therefore, the bandpass filter is always centered at the BPF tone. The BPF tone is then processed to obtain its power, i.e. mean-square-value. Though extracting the BPF tone signal can also be achieved using adaptive digital techniques [7], the main advantage is the very low cost of the analog components as compared to digital signal boards. This approach has been successfully implemented on the control of high-cycle-fatigue of engine blades [8].

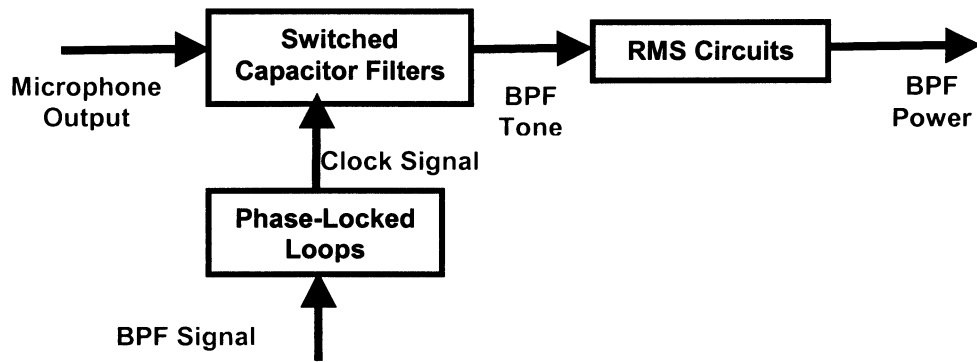


Figure 3.18: BPF tone extractor system.

The performance of the BPF tone extractor is demonstrated in figures 3.19 and 3.20. The time histories of one of the original microphone signals and the BPF tone component (after the BPF extractor) are shown in figure 3.19. The corresponding frequency spectra are shown in Figure 3.20. This figure clearly indicates that only the BPF tone signal is filtered out while the broadband component is almost completely rejected. These results clearly demonstrate the very good performance of the analog BPF extractor circuit.

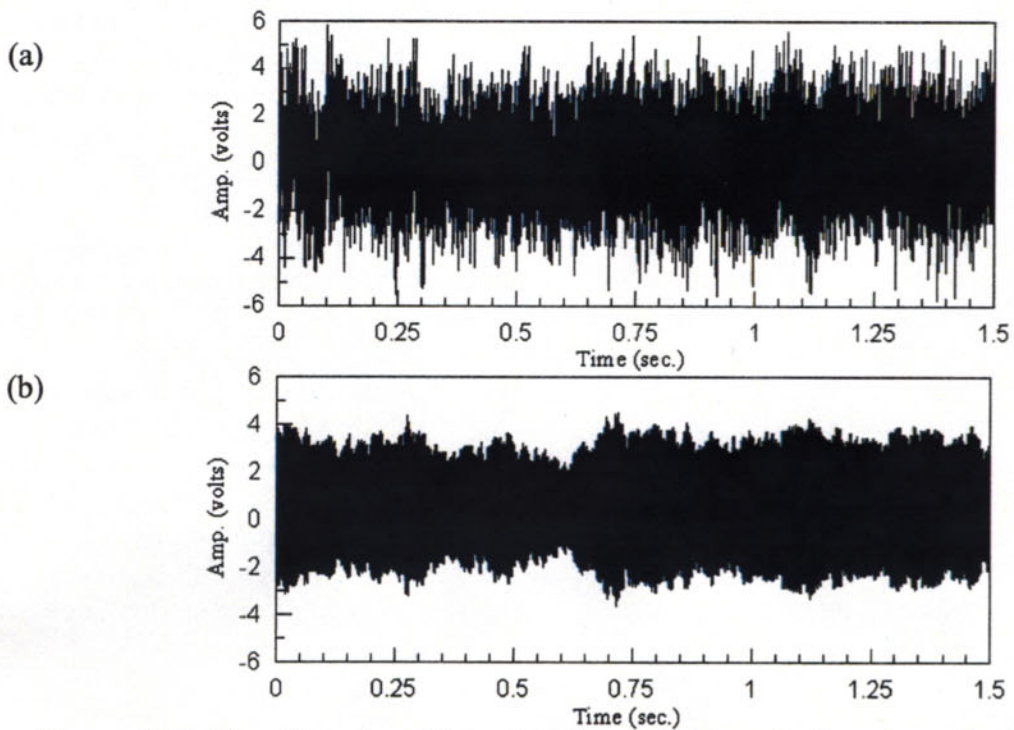


Figure 3.19: Time histories of (a) original and (b) filtered microphone, i.e. BPF tone, signals.

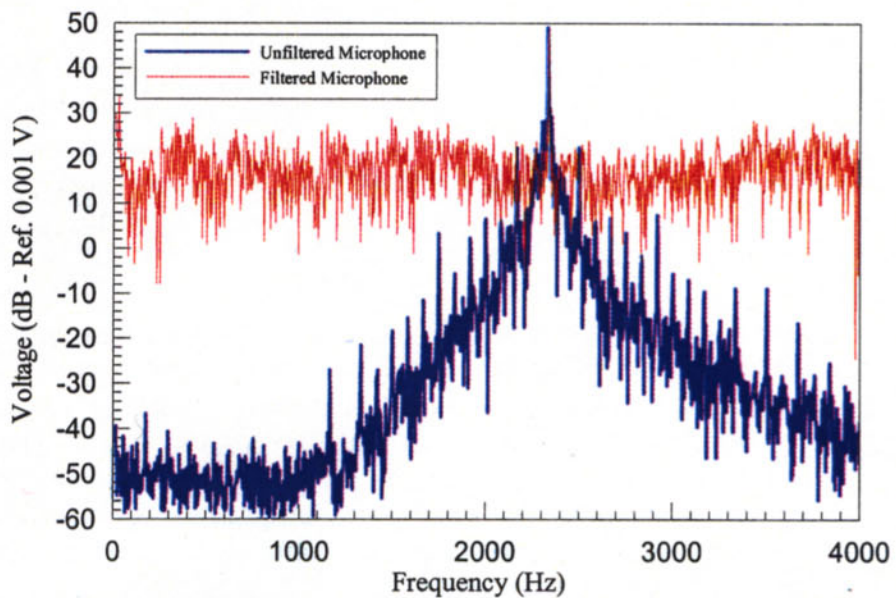


Figure 3.20: Spectrum of (a) original and (b) filtered microphone signals

The BPF tone components from the microphones were then used to estimate the acoustic power radiated over the sector in the far-field where the error microphones were located. The microphone BPF tone signals were digitized and the mean-square-values estimated using a moving average approach. The mean-square-value signals were then added to give an estimate of the sound power, i.e. error signal to be minimized.

To investigate the effect of the tube length over the BPF tone power estimate, the error signal was plotted as a function of the tube length at three engine speeds resulting in BPF tone frequencies of 2225, 2350, and 2400 Hz, respectively. The sound power radiated over the selected sector in the far-field (error signal) as a continuous function of the tube length is plotted in figures 3.21a-c for the three BPF tone frequencies. To determine the attenuation as a function of the tube length, the error signal was also recorded for the hard wall case for the same three BPF tone frequencies. The hard wall error signal is indicated by the red line in figures 3.21a-c and it is obviously not a function of tube length. It is important to remark that the error signal was not calibrated and thus the levels are not indicative of actual sound power levels. However, the reduction of the error signal is the reduction in sound power radiated over the monitored sector.

It is very clear in these figures that there exists an optimum tube length for the system at each BPF tone. It is interesting to observe that for the BPF tone frequency of 2350 Hz there is a relatively narrow range of tube lengths that leads to the best attenuation. In contrast the other two frequencies show that the range of tube length that results in good BPF tone reduction is not as sensitive as before. It is possible that the behavior at the extreme frequencies shown is because the true optimum is outside the range of tube length implemented here.

The next experiments consisted of demonstrating the performance of the adaptive control concept. To this end, a simple control algorithm was developed that changed the tube length to minimize the error signal, e.g. BPF tone power estimate. The control algorithm simply searched the minimum of the error signal (cost function) by evaluating its slope (gradient search technique).

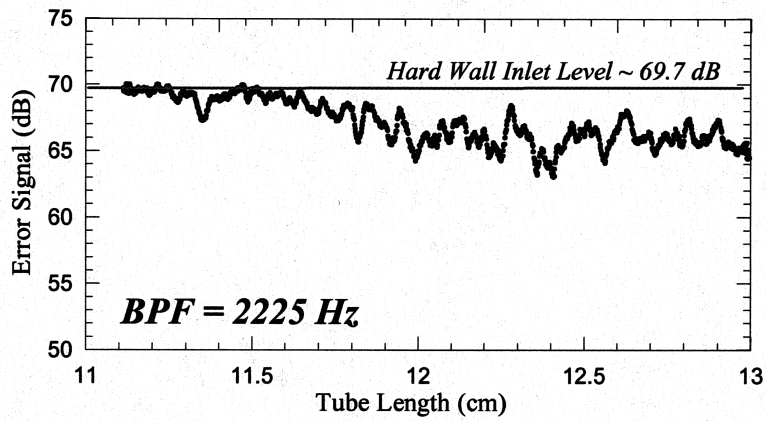
The experimental results from the adaptive control test are presented in figures 3.22a-c. The JT15D engine was started and set to operate such that the engine speed was around 2400 Hz. Then the engine speed was reduced until the BPF tone frequency was down to about 2250 Hz over several minutes. During this time, the error signal, tube length, and BPF tone frequency time histories were recorded and are shown in figures 3.22a through 3.22c. Figure 3.22c shows that over the first 60 seconds, the engine speed was kept approximately constant to yield a BPF tone of 2400 Hz. The initial tube length was set at 12.6 cm which is not close to the optimum length for this frequency (see figure 3.21). It is clear from figure 3.22b that the controller adjusted the tube length to the optimum value of 11.1 cm in about 40 seconds. Soon after the controller adjusted the tube length, the engine speed was slowly decreased as shown in figure 3.22c. The controller kept adjusting the HQ-system by increasing the tube length. The symbol (●) in figure 3.22 indicates an estimate of the optimum tube length at the corresponding BPF tone

frequency obtained from figures 3.21 a-c.

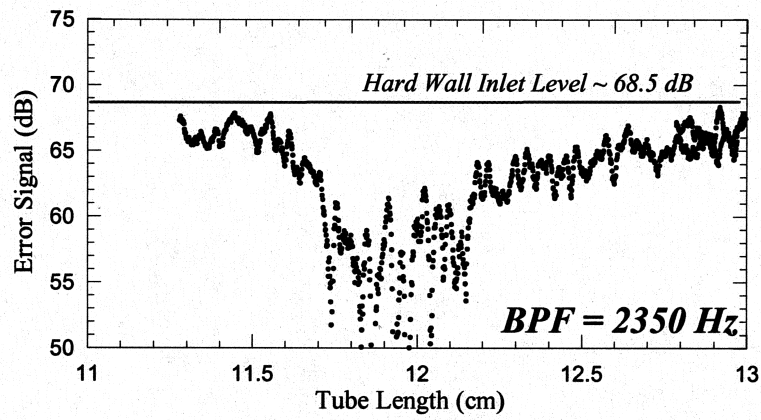
Finally the performance of the adaptive HQ-system is validated from the results in figure 3.22a. In this figure, the time history of the error signal is shown for the adaptive HQ-system. To determine the attenuation of the error signal, the error signal for the hard wall case as a function of the BPF tone frequency is plotted as a continuous red line. It is clear that the adaptive system was capable of maintaining a reduction of more than 6 dB on the error signal, and thus of the radiated power over the sector where the error microphones are located, over most of the 6 minutes of testing time.

The results from this adaptive HQ-system experiment clearly demonstrate the potential benefits of adjusting the HQ-properties to optimize its performance over a range of frequencies. The control system it has a very slow response time. However, the control algorithm selected for this first set of experiments was very simple and can be improved. In addition, a real implementation will probably not require a very fast time response for the system.

(a)



(b)



(c)

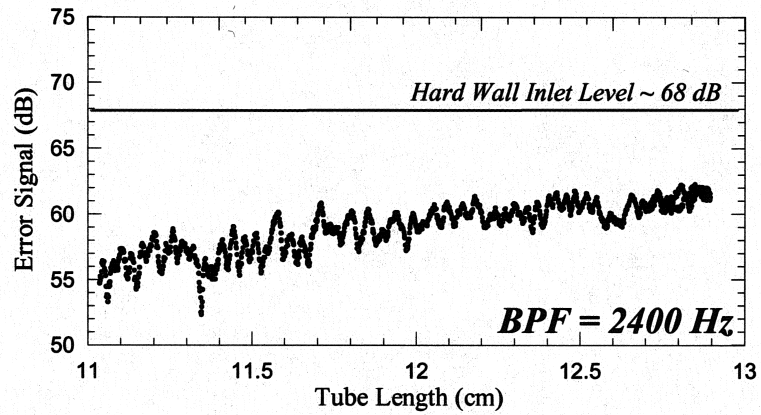
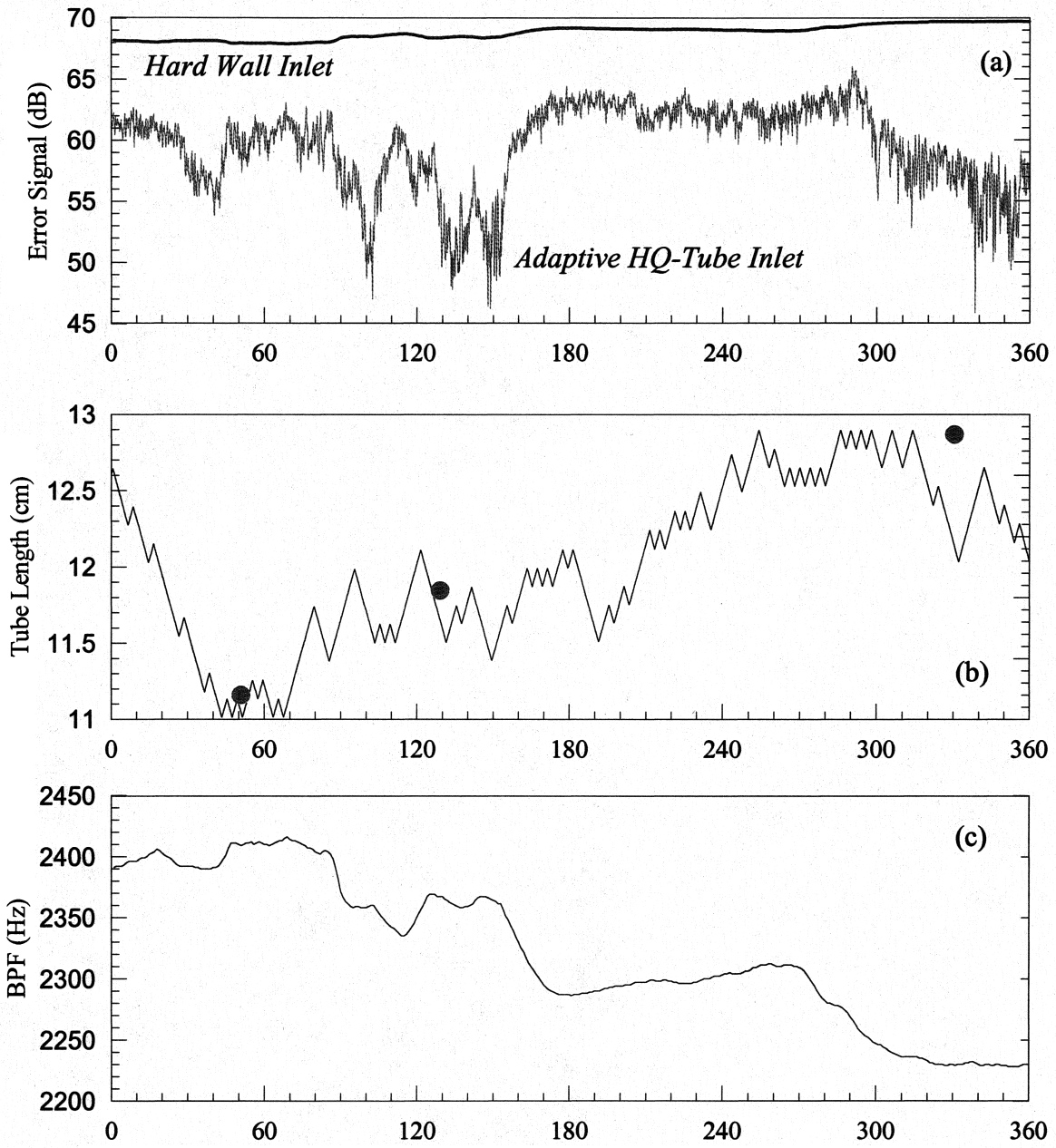


Figure 3.21: Estimated power by error-microphones as a function of tube length at (a) 2225, (b) 2350, and (c) 2400 Hz.



4. CONCLUSIONS

In general, the experiments performed on the JT15D demonstrate that the application of HQ tubes to the problem of turbofan jet engine noise is a very effective and viable strategy. In this section, the main conclusions obtained from the research performed in this experimental part of the research endeavor are discussed.

The first part of this report showed the experimental results obtained with one and two arrays of Herschel-Quincke (HQ) tubes installed on the JT15D engine inlet, with the engine configured without excitation rods. All previous tests with the HQ tubes were performed with 27 rods located upstream of the fan [1] that resulted in the $m=1$ circumferential order mode to dominate the inlet sound field. These tests performed without the rods resulted in the $m=5$ circumferential order mode to dominate the inlet sound field. Both broadband and tonal data were obtained for a hard-walled inlet and for the inlet configured with one and two arrays of HQ tubes. The good attenuation of the broadband and BPF tone components once again demonstrated the potential of the HQ-concept.

The second part of the report described the efforts to develop adaptive capabilities for the HQ-system. A preliminary investigation into the potential of using adaptive HQ tubes was presented. It is clear that although the tubes are very effective over a range of BPFs, there is an optimal BPF at which the best attenuation occurs. This implies that in order to optimize the attenuation effect of the tubes over a wide range of BPF tones, the tubes should be adapted to “track” the BPF as it changes. Two adaptation mechanisms were proposed and built. One approach consisted of using a “flap” placed at the center of the tube. It was shown that this flap changed the 2nd resonance of the tube without affecting the first one. The second approach consisted of changing the tube length using expandable elements. This technique demonstrated that adjusting the tube length shifts both the 1st and 2nd tube resonances. This last adaptation mechanism was also implemented in conjunction with an adaptive control algorithm. Three microphones were placed in the far-field and used to estimate the power radiated over a sector. The control algorithm adjusted the tube length to minimize this power estimate as the engine speed was changing. One of the main conclusions of the work on the adaptive-HQ concept is that adaptation of the HQ-tubes to optimize performance is feasible. However, the frequency range in which the adaptive system can operate is probably limited, e.g. 10% of the BPF tone. Thus, the potential application of an adaptive HQ-system might be in optimizing the performance for a single engine power setting, i.e. approach, cutback, and so forth. It would be difficult to device an adaptive HQ-system that can be adjusted to optimally work at more than one power setting.

5. RECOMMENDATIONS FOR FUTURE RESEARCH

The adaptive HQ-system is an approach that needs to be further investigated. One of the most important issues is to determine the practical conditions under which the adaptation concepts would be most beneficial. It is obvious that much work is needed in

practical adaptation mechanisms, in particular for mechanisms that do not require moving parts. Some options include affecting the tube acoustics through flow injection (similar to bias-flow in liners) or temperature gradients.

Another area of research for the implementation of adaptive HQ-systems is in the development of sensing concepts and control algorithms. The development of control algorithms is probably not critical since there are numerous techniques that can be implemented in this application. However, the sensing concept requires further research efforts. To adjust the tube properties, it is important to obtain "error" information that relates to the inlet radiated acoustic power. One feasible approach is to place axial arrays of microphones on the inlet wall to estimate the radiated power over far-field sectors using wavenumber concepts [9,10].

ACKNOWLEDGEMENTS

This work was supported by the Aeroacoustics Branch of the NASA Langley Research Center which is gratefully acknowledged. The technical monitors for this work are Dr. Carl Gerhold and Dr. Joe Posey.

REFERENCES

- [1] Smith, J. P. and Burdisso, R. A., "The Application of the Herschel-Quincke Tube Concept for the Reduction of Tonal and Broadband Noise From Turbofan Engines," VPI report VPI-ENGR.98.167, prepared for NASA under grant # NAG-1-1980 and proposal # 98-0448-10, 1998.
- [2] Preisser, J. S., Schoenster, J. A., Golub, R. A., and Horne, C., "Unsteady Fan Blade Pressure and Acoustic Radiation From a JT15D-1 Turbofan Engine at Simulated Forward Speed," AIAA Paper 81-0096 presented at the 19th Aerospace Sciences Meeting, January 12-15, 1981.
- [3] Burdisso, R. A., Thomas, R. H., Fuller, C. R., and O'Brien, W. F., "Active Control of Spinning Modes from a Turbofan Engine," AIAA Journal, Vol. 32, No. 1, pp.23-30, 1994.
- [4] Burdisso, R.A., Fuller, C.R., Smith, J.P., "Experiments on the Active Control of a Turbofan Inlet Noise using Compact, Lightweight Inlet Control and Error Transducers," CEAS/AIAA-95-028, 1995, pp. 177-185.
- [5] Smith, J.P., Burdisso, R.A., and Fuller, C.R., Experiments on the Active Control of Inlet Noise From a Turbofan Jet Engine Using Multiple Circumferential Control Arrays, AIAA 96-1792, 1996.

- [6] Homyak, L., McArdle, J. G., and Heidelberg, L. J., "A Compact Inflow Control Device for Simulating Flight Fan Noise," AIAA Paper no. 83-0680 presented at the AIAA 8th Aeroacoustic Conference, April 11-13, 1983.
- [7] Widrow B. and Stearns S. D., "Adaptive Signal Processing," Prentice-Hall Signal Processing Series, Englewood Cliffs, N.J., 1985.
- [8] J. Feng, J. Kozak, T. Bailie, R. A. Burdisso and W. N. Ng, "Active Flow Control Using Microphone Sensors to Reduce Fan Noise," AIAA-2000-1993, 6th AIAA/CEAS Aeroacoustics Conference, Maui, Hawaii, USA, 12-14 June 2000.
- [9] Smith J. P. and Burdisso R. A., "Active Control of Inlet Noise from a Turbofan Engine Using Inlet Wavenumber Sensors," 5th AIAA/CEAS Aeroacoustics Conference AIAA 99-1808, Seattle, Washington, USA, 10-12 June 1999.
- [10] Smith J. P., Burdisso R. A., Sutliff D.L., and Heilderberg L. J. "Active Control on a Large-scale Ducted Fan Inlet With Wavenumber Sensing," *139th Meeting of the Acoustical Society of America*, Atlanta, Georgia, May 31 2000.

REPORT DOCUMENTATION PAGE

Form Approved
OMB No. 0704-0188

Public reporting burden for this collection of information is estimated to average 1 hour per response, including the time for reviewing instructions, searching existing data sources, gathering and maintaining the data needed, and completing and reviewing the collection of information. Send comments regarding this burden estimate or any other aspect of this collection of information, including suggestions for reducing this burden, to Washington Headquarters Services, Directorate for Information Operations and Reports, 1215 Jefferson Davis Highway, Suite 1204, Arlington, VA 22202-4302, and to the Office of Management and Budget, Paperwork Reduction Project (0704-0188), Washington, DC 20503.

1. AGENCY USE ONLY (Leave blank)		2. REPORT DATE March 2002	3. REPORT TYPE AND DATES COVERED Contractor Report	
4. TITLE AND SUBTITLE Experiments With Fixed and Adaptive Herschel-Quincke Waveguides on the Pratt and Whitney JT15D Engine			5. FUNDING NUMBERS G NAG1-2137 WU 706-81-12-01	
6. AUTHOR(S) Jerome P. Smith Ricardo A. Burdisso				
7. PERFORMING ORGANIZATION NAME(S) AND ADDRESS(ES) Virginia Polytechnic Institute and State University Department of Mechanical Engineering Blacksburg, VA 24061			8. PERFORMING ORGANIZATION REPORT NUMBER VPI-ENGR 4-26483	
9. SPONSORING/MONITORING AGENCY NAME(S) AND ADDRESS(ES) National Aeronautics and Space Administration Langley Research Center Hampton, VA 23681-2199			10. SPONSORING/MONITORING AGENCY REPORT NUMBER NASA/CR-2002-211430	
11. SUPPLEMENTARY NOTES NASA Langley Technical Monitor: Carl H. Gerhold				
12a. DISTRIBUTION/AVAILABILITY STATEMENT Unclassified-Unlimited Subject Category 71 Availability: NASA CASI (301) 621-0390			12b. DISTRIBUTION CODE	
13. ABSTRACT (Maximum 200 words) This report summarizes the key results obtained by the Vibration and Acoustics Laboratories at Virginia Tech over the period from January 1999 to December 2000 on the project "Investigation of an Adaptive Herschel-Quincke Tube Concept for the Reduction of Tonal and Broadband Noise from Turbofan Engines", funded by NASA Langley Research Center. The Herschel-Quincke (HQ) tube concept is a developing technique the consists of circumferential arrays of tubes around the duct. A fixed array of tubes is installed on the inlet duct of the JT15D research engine at Virginia Tech. In addition, an adaptive configuration is evaluated in which the H-Q noise control system is optimized by changing the parameters of the tubes as the engine speed is varied.				
14. SUBJECT TERMS duct propagation, experiment, turbofan, Herschel-Quincke tube			15. NUMBER OF PAGES 40	
			16. PRICE CODE	
17. SECURITY CLASSIFICATION OF REPORT Unclassified	18. SECURITY CLASSIFICATION OF THIS PAGE Unclassified	19. SECURITY CLASSIFICATION OF ABSTRACT Unclassified	20. LIMITATION OF ABSTRACT UL	

